PHYSICAL REVIEW B **99**, 140505(R) (2019)

Rapid Communications

Vorticity and quantum turbulence in the merging of superfluid helium nanodroplets

José María Escartín,[1] Francesco Ancilotto,[2,3] Manuel Barranco,[4,5,6] and Martí Pi[4,5]

[1]*Theory of Condensed Matter Group, Cavendish Laboratory, University of Cambridge, 19 JJ Thomson Avenue, Cambridge CB3 0HE, United Kingdom*

[2]*Dipartimento di Fisica e Astronomia "Galileo Galilei" and CNISM, Università di Padova, via Marzolo 8, 35122 Padova, Italy*

[3]*CNR-IOM, via Bonomea, 265–34136 Trieste, Italy*

[4]*Departament de Física Quàntica i Astrofísica, Facultat de Física, Universitat de Barcelona, Av. Diagonal 645, 08028 Barcelona, Spain*

[5]*Institute of Nanoscience and Nanotechnology (IN2UB), Universitat de Barcelona, Barcelona, Spain*

[6]*Université Toulouse 3, Laboratoire des Collisions, Agrégats et Réactivité, IRSAMC, 118 route de Narbonne, 31062 Toulouse Cedex 09, France*

(Received 14 February 2019; published 16 April 2019)

We have studied the merging of two identical ^{4}He droplets at zero temperature, caused by their van der Waals mutual attraction. During the early stages of the merging, density structures appear which closely match the experimental observations by Vicente *et al.* [J. Low Temp. Phys. **121**, 627 (2000)]. When the droplets are merging, quantized vortex-antivortex ring pairs nucleate at the surface and annihilate inside the merged droplet producing a roton burst. We also observe the nucleation of quantized vortex-antivortex rings that wrap the droplet surface and remain localized on the surface until they eventually decay into short-wavelength surface waves. Analysis of the kinetic energy spectrum discloses the existence of a regime where turbulence caused by vortex interaction and annihilation is characterized by a Kolmogorov power law. This is followed by another regime where roton radiation—produced by vortex-antivortex annihilation—dominates, whose hallmark is a weak, turbulent surface dynamics. We suggest that similar processes might appear in superfluid helium droplets after they capture impurities or if they are produced by hydrodynamic instability of a liquid jet. Experiments on collisions between recently discovered self-bound Bose-Einstein condensates should display a similar phenomenology.

DOI: 10.1103/PhysRevB.99.140505

Superfluid helium droplets are fascinating objects that have drawn the interest of both experimentalists and theoreticians [1]. This interest is notoriously broad and includes, e.g., the nature of superfluidity at the nanoscale, the interaction of atomic and molecular impurities with the hosting droplets, and the study of vortical states in nanodroplets (see Refs. [2,3] for recent comprehensive reviews).

One of the hallmarks of superfluidity is the appearance of quantized vortices [4,5]. Whereas the presence of vortices in macroscopic samples of bulk liquid helium was unambiguously proved long ago, in the case of helium droplets it remained elusive. It is only recently that vortex arrays inside droplets made of 10^8–10^{11} atoms were detected by coherent x-ray scattering [6].

The coalescence of superfluid ^{4}He drops of several tenths of centimeter radius levitating in a magnetic trap was investigated some time ago [7]. The experimental setup allowed one to study their merging at fairly low velocity, and the temperature was kept low enough to make the helium vapor around them negligible, so that the droplets were essentially isolated.

In this work we address the coalescence of two identical ^{4}He droplets drawn together by the mutual van der Waals (vdW) long-range attraction. After showing that the merging yields density structures which closely match the experimental observations even in their fine details, we show that vorticity nucleates both inside and on the surface of the merged droplet. The subsequent decay of vorticity results in the appearance of two distinct turbulence regimes, which we characterize with their kinetic energy spectra. Multimedia content is provided as Supplemental Material [8].

We study the strongly correlated superfluid ^{4}He by using a realistic density functional theory (DFT) approach which allows one to reproduce complex dynamical phenomena such as vortex nucleation and vortex-density wave interactions [2]. One important outcome of our simulations is an accurate description of the dynamics of vortex interactions and annihilation, which is a fundamental ingredient of current studies of quantum turbulence in liquid He and in cold-gas superfluids [9–12].

The Gross-Pitaevskii (GP) approach [5] has been also shown to be capable to sustain these phenomena. Vortex ring emission and the possible transition to a chaotic turbulent regime due to vortex interactions and decay has been studied within time-dependent GP theory in both superfluid ^{4}He and Bose-Einstein condensates (BECs) [4,13–18]. It is well known, however, that GP theory cannot provide an accurate description of the vortex core structure in superfluid liquid helium, and can at most reproduce the phonon part of the ^{4}He dispersion relation. In the following, we will prove the role of roton emission in turbulence phenomena in ^{4}He, and we will show that the roton wave vector provides indeed a natural dividing line between the different length scales contributing to the turbulence created by the droplet collision process.

Within DFT, the total energy of a ^4He_N droplet at zero temperature is written as a functional of an effective wave function $\Psi(\mathbf{r}, t)$ related to its atomic density by $\rho(\mathbf{r}, t) = |\Psi(\mathbf{r}, t)|^2$. In this study, the number of helium atoms in each of the initial droplets is $N = 500$, and the results we present have been obtained using the 4HE-DFT BCN-TLS computing package [19]. The density functional used in this work is finite range and includes nonlocal effects [20], since both aspects are needed to describe quantitatively the response of the liquid at the scale of the vortex core radius, which is of the order of 1 Å [21]. This functional reproduces quite faithfully the density modulations around the vortex core [2]. These modulations have been interpreted as a cloud of bound virtual rotons embodied in the phase of the vortex wave function, and they may be converted into real ones following vortex-antivortex annihilations, making vortex tangles a potential source of nonthermal rotons [22]. Our simulations provide clear evidence of such conversion process.

We have first determined the equilibrium configuration of an isolated helium droplet by solving the static DFT problem [2]. These droplets are spherical, and their sharp density surfaces, defined as the locus where the helium density equals half the bulk liquid value $\rho_0 = 0.0218$ Å^{-3}, have a radius $R = r_0 N^{1/3}$ with $r_0 = 2.22$ Å. The energy of the $^4He_{500}$ droplet is -2474.6 K, and that of the $^4He_{1000}$ droplet is -5400.3 K. An energy of 451.2 K, mainly arising from the decrease of surface energy [23], is thus available for the merging.

Next, we place the droplets at rest so that their surfaces are about 6 Å away from contact, and use this as the initial configuration for the merging dynamics within the time-dependent DFT (TDDFT) approach. This is in stark contrast with classical calculations of merging, since they have to start from two sharp surfaces with a point of contact and to assume that by some microscopic mechanism a tiny bridge appears joining the droplets [24]; and with BEC calculations of confined [25] or self-sustained droplets, where some velocity has to be given to the droplets to trigger the collision [26]. In our case, it is the vdW mutual attraction that provides such a microscopic mechanism.

The TDDFT equation [2,19] has been solved up to $t = 600$ ps with a time step $\Delta t = 1$ fs. Droplet coalescence proceeds by the development of a tiny, low-density bridge connecting the droplets in about 4.5 ps [8]. Figure 1 displays the linear t dependence of the squared neck radius $R^2_{\rm neck}$ with 6.31 Å^2/ps slope, showing that $R_{\rm neck} \propto t^{1/2}$. In spite of the different length and time scales, the same behavior has been observed in experiments on low-viscosity fluids [27]. Calculations for classical droplets yielded [24,28]

$$\frac{R_{\rm neck}}{R} = \beta\sqrt{\frac{t}{\tau}} \tag{1}$$

with $\tau = (\rho R^3/\sigma)^{1/2}$, where ρ is the mass density of the fluid, σ its surface tension, and R is the droplet's radius. The β factor was calculated for inviscid droplets yielding a value of 1.62 [28], while measurements gave values in the 1.03–1.29 range [27]. Using for τ the liquid ^{4}He value and the calculated slope, we find $\beta = 0.93$. We have analyzed the first few frames of Fig. 2 in Ref. [7], also finding $R_{\rm neck} \propto t^{1/2}$ but with a significantly higher prefactor, $\beta = 6.75$. This discrepancy is attributed to the different impact velocity of the droplets, which is zero in our case and a few cm/s in the experiment [7].

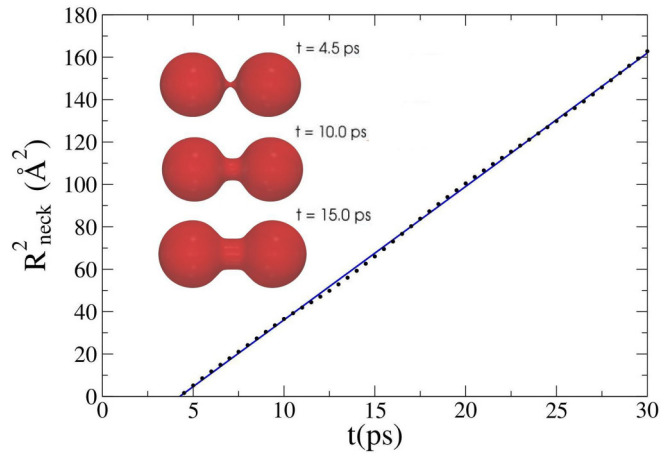

FIG. 1. Time evolution of $R^2_{\rm neck}$. Also shown are several droplet configurations at the labeled times.

The droplets eventually merge, producing in the process two protrusions symmetrically placed along the collision direction, as shown in Fig. 2 for $t = 92$ ps. The growth of the merging neck and the appearance of the protrusions at the droplet surface displayed in Fig. 2 are remarkably similar to those found for the coalescence of ^{4}He drops of 0.20–0.25 cm radius, as shown in Fig. 2 of Ref. [7], with the only obvious differences being the time and length scales involved.

As the protrusions shrink, pairs of quantized vortex-antivortex rings are nucleated at the necks that connect the protrusions with the merged droplet, with all vortex (antivortex) rings located around the left (right) neck. Once formed, the rings of each pair move symmetrically toward the droplet

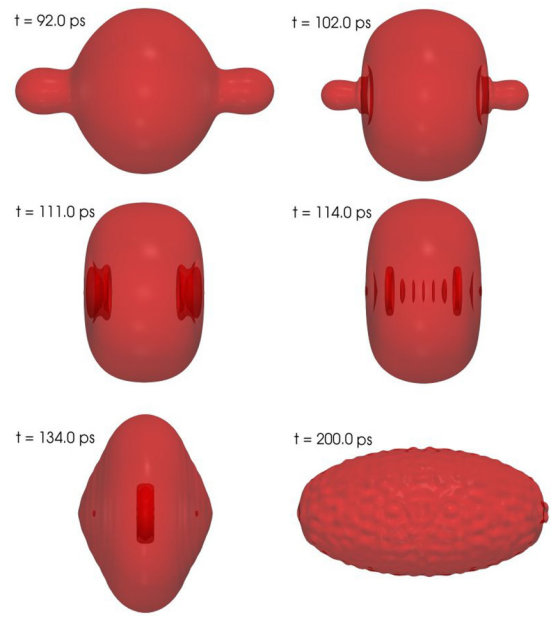

FIG. 2. Sharp density surfaces, at the labeled times, in the merging of two $^4He_{500}$ droplets.

center [8]. Two such vortex-antivortex pairs can be identified in Fig. 2 at $t = 111$ ps. Additionally, lenticular, sharp density indentations appear in the regions between rings, likely shock waves produced by the sudden collapse of the protrusions; these indentations are separated by a distance similar to that between He atoms in the compressed liquid.

During their motion, the smaller radius rings catch up to the larger radius rings and pass through them, shrink, and eventually disappear at $t \simeq 114$ ps. The larger radius vortex-antivortex rings last up to $t \simeq 139$ ps, when they collide against each other and annihilate, producing a roton burst (as explained in the following). We may estimate the energy ΔE released in the annihilation event by recalling that, in ^{4}He, the energy of a vortex ring of radius R_v is $E_v = (2\pi^2\hbar^2/m)\rho_0 R_v[\ln(8R_v/a) - 1.615]$ [29], where $a = 0.7$ Å is the vortex core size. In our case, the vortex ring radius just before annihilation is $R_v \sim 8$ Å, which leads to $\Delta E = 2E_v \sim 240$ K. This corresponds to the emission of ∼24 rotons [30].

In the later stages of the time evolution, the droplet appears to be in a highly excited state characterized by short-wavelength nanoscopic surface waves, as shown in Fig. 2 at $t = 200$ ps. Similar surface patterns have been found in the decay of multicharged vortices in trapped BEC [31]. Superposed to this complex surface dynamics, the merged droplet undergoes large amplitude oscillations, its shape periodically shifting from oblate to prolate [8].

The presence of quantized vortices in the droplet during the merging, their mutual interaction, and their annihilation followed by the emission of rotons, is likely a source of turbulence, which we address here with the aid of a widely used tool in studies of classical and quantum turbulence, i.e., the kinetic energy spectrum whose dependence upon the wave number k allows one to distinguish different regimes that are relevant for characterizing turbulence [10].

Writing the effective wave function as $\Psi(\mathbf{r},t) = \sqrt{\rho(\mathbf{r},t)}\exp[\imath\mathcal{S}(\mathbf{r},t)]$, the atom current density is $\mathbf{j}(\mathbf{r},t) = \rho(\mathbf{r},t)\mathbf{v}(\mathbf{r},t)$ with $\mathbf{v}(\mathbf{r},t) = \hbar\nabla\mathcal{S}(\mathbf{r},t)/m$. Thus, the kinetic energy of the superfluid can be written as

$$E_{\rm kin}(t) = \frac{\hbar^2}{2m}\int d\mathbf{r}\,|\nabla\sqrt{\rho(\mathbf{r},t)}|^2 + \frac{m}{2}\int d\mathbf{r}\,\frac{\mathbf{j}^2(\mathbf{r},t)}{\rho(\mathbf{r},t)}. \quad (2)$$

The first term is the quantum pressure while the second is the usual hydrodynamic kinetic energy $E_{\rm hyd}$. Working in Fourier space, one can rewrite $E_{\rm hyd}$ as

$$E_{\rm hyd}(t) = 4\pi\int_0^\infty dk\,\mathcal{E}_{\rm hyd}(k,t), \quad (3)$$

where the energy spectrum $\mathcal{E}_{\rm hyd}(k,t)$ is the spherical average in $\mathbf{k}$ space [4,32,33]

$$\mathcal{E}_{\rm hyd}(k,t) = \frac{m}{2}(2\pi)^3\frac{k^2}{4\pi}\int_{\Omega_k} d\Omega_k\left|\frac{\widetilde{\mathbf{j}}}{\sqrt{\rho}}(\mathbf{k},t)\right|^2. \quad (4)$$

We have decomposed it into a divergence-free (incompressible) part, related to vorticity, and a compressible part [32], related to density waves, and have analyzed them separately [34].

Figure 3 shows both additive components of $\mathcal{E}_{\rm hyd}(k,t)$, as well as three relevant k values: $k_{\rm vort} = 2\pi/a = 6.3$ Å^{-1},

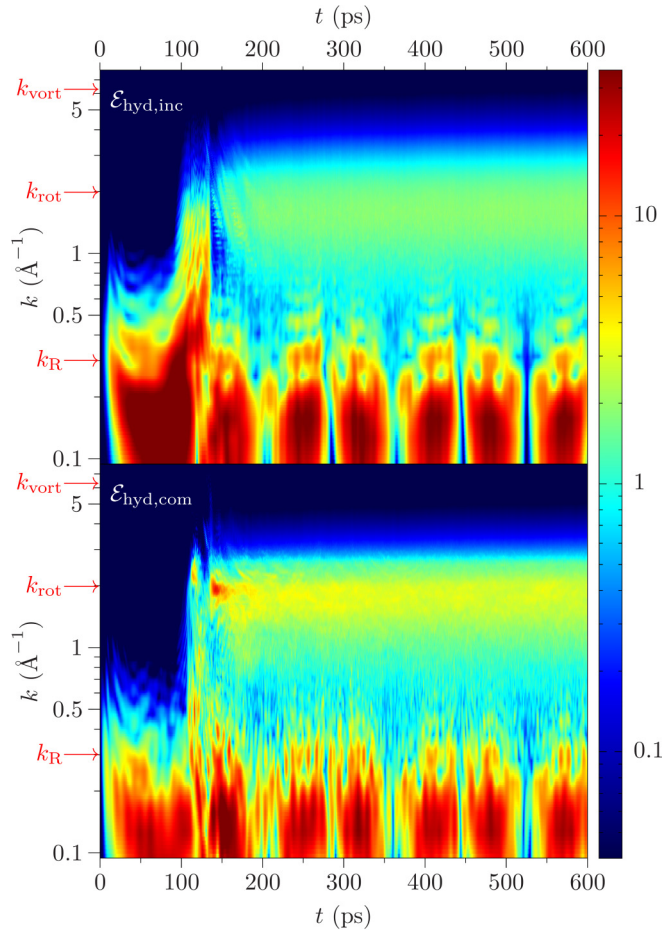

FIG. 3. Energy spectrum $\mathcal{E}_{\rm hyd}(k,t)$ (K Å). Top: incompressible part; bottom: compressible part.

a being the vortex core size ∼1 Å; $k_{\rm R} = 2\pi/R = 0.3$ Å^{-1}, where R is the radial dimension of the droplet, and the roton wave vector $k_{\rm rot} = 1.98$ Å^{-1}. Both components periodically display bright regions in the small k region ($k \lesssim k_{\rm R}$) in phase with the oscillations of the shape of the merged droplet. Interestingly, in the compressible part (bottom panel), a bright peak appears at $t \simeq 140$ ps corresponding to the roton burst created by the annihilation of the large vortex-antivortex rings. This peak spreads with time and is present in the rest of the simulation [35]. The fainter spot at $t \simeq 115$ ps originates from the mentioned large amplitude density waves that appear between the larger vortex and antivortex rings.

Between approximately 100 and 140 ps, the relevant part of the incompressible energy spectrum is dominated by the presence of vortices and their decay (top panel of Fig. 3). The top panel of Fig. 4 corresponds to this regime. It displays two powers laws, $k^{-3.00}$ and $k^{-1.64}$, which are strikingly similar, respectively, to that arising from the presence of vortices [32,33], and to the Kolmogorov classical scaling, $k^{-5/3}$, which is known to be also present in bulk superfluid turbulence [32,36].

At later times, the compressible part of the energy spectrum is dominated by rotons and their effect on the droplet surface (see below). The bottom panel of Fig. 3 corresponds to this regime, whose scaling laws are shown in the bottom panel of

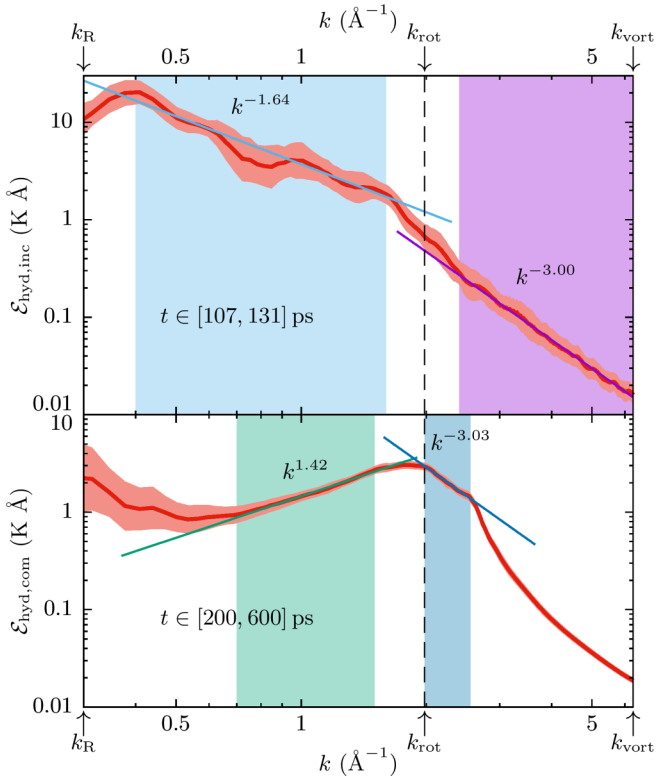

FIG. 4. Power-law analyses of time averages of the incompressible (top panel) and compressible (bottom panel) energy spectra. Each of the two panels displays, in log-log scales, the time-averaged spectrum $\mathcal{E}(k)$ (red line) and the range within a standard deviation (light red) for every k, as well as the corresponding power laws determined by weighted fits over the shadowed k intervals and indicated time intervals. Top panel: $k^{-1.64\pm0.05}$ for $k \in [0.4, 1.6]$ Å^{-1} (light blue) and $k^{-3.00\pm0.01}$ for $k \in [2.4, 2\pi]$ Å^{-1} (violet). Bottom panel: $k^{1.42\pm0.02}$ for $k \in [0.70, 1.50]$ Å^{-1} (green) and $k^{-3.03\pm0.05}$ for $k \in [1.98, 2.55]$ Å^{-1} (dark blue).

Fig. 4. It is the analog of the weak-wave turbulence regime arising from acoustic radiation, characterized by a $k^{-3/2}$ law [10,37], although other scalings, such as $k^{-7/2}$, have also been found [34]. In our case, the spectrum displays two power laws with exponents 1.42 and −3.03. One might expect that the scalings associated to droplet surface turbulence are not those of two-dimensional turbulence on a flat surface [10,34,37]. Moreover, since the wave energy spectrum depends on the size and shape of the droplet surface, one should not expect a universal behavior.

Inspection of the early stages of superfluid flow passing through the neck connecting the two merging droplets shows that the circulation lines have a tendency to bend outward at the contact region, hinting at the possible nucleation of vortex-antivortex rings on the outer droplet surfaces, which cannot be observed by the mere inspection of the droplet densities [8]. To help identify the presence of vorticity in these low-density regions, we have calculated the pseudovorticity $\nabla \times \mathbf{j}(\mathbf{r}, t)$ [38]. Plots of $|\nabla \times \mathbf{j}(\mathbf{r}, t)|$ isosurfaces allow one to visualize regions of potentially nonzero vorticity [39].

A video in the Supplemental Material [8] shows how pseudovorticity spreads and slips on the outer surface of the merging droplets, and Fig. 5 displays pseudovorticity isosurfaces for selected times. We have checked that, between 12 and 90 ps, the circulation around the more intense of these tiny surface structures is quantized, with charges ±1, hence signaling bona fide vortex/antivortex rings [40]. These vortices do not sink into the droplet but remain on the surface (shells of parallel ringlike structures appearing in Fig. 5). Eventually, they decay and fragment due to the nanoscopic indentations appearing on the surface of the merged droplet at $t \sim 160$ ps, when the surface changes its appearance from smooth to rough [8], thus causing the weak-wave turbulence discussed before. Superfluid helium droplets, after capturing impurities [2] or being produced by hydrodynamic instability of a liquid jet [6], might experience a similar process.

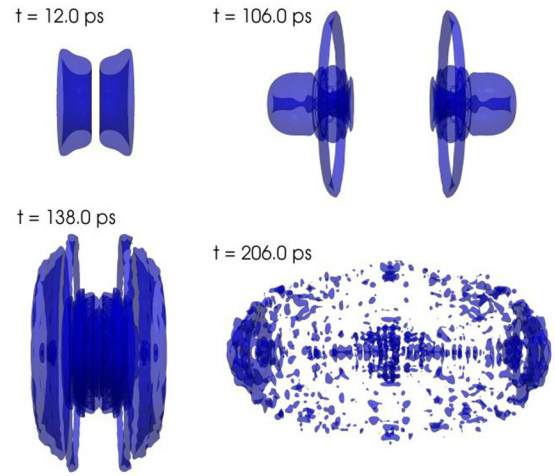

FIG. 5. Pseudovorticity in the merging of two ^{4}He$_{500}$ droplets, visualized by $|\nabla \times \mathbf{j}(\mathbf{r}, t)| = 10^{-3}$ Å^{-3} ps^{-1} isosurfaces at the labeled times.

Although most of the pseudovorticity appearing when $t >$ 160 ps is localized on the droplet surface region, lenticular patterns remain in its bulk. These patterns, which are remnants of the sharp density indentations discussed before, can be seen, e.g., in Fig. 5 at $t = 206$ ps, where a train of such faint structures is visible along the incident direction.

Finally, we would like to mention that recent realizations of stable self-bound ultradilute quantum droplets, made of atoms of a binary mixture of BECs [41,42], allow one to address droplet merging in a different superfluid environment [26] and in a likely more controllable way, opening up the possibility of studying wave turbulence on their surfaces. Self-bound BEC droplets made of dipolar gases displaying a roton minimum [43] might also disclose nonthermal roton emission in these systems.

We thank Humphrey Maris, Luciano Reatto, Jussi Eloranta, Alessio Recati, and Albert Gallemí for useful exchanges and discussions. This work has been performed under Grant No. FIS2017-87801-P (AEI/FEDER, UE). M.B. thanks the Université Fédérale Toulouse Midi-Pyrénées for financial support through the "Chaires d'Attractivité 2014" Programme IMDYNHE. J.M.E. acknowledges financial support from the Engineering and Physical Sciences Research Council, UK, under Grant No. EP/P034616/1.

[1] J. P. Toennies and A. F. Vilesov, Angew. Chem. Phys. **43**, 2622 (2004).

[2] F. Ancilotto, M. Barranco, F. Coppens, J. Eloranta, N. Halberstadt, A. Hernando, D. Mateo, and M. Pi, Int. Rev. Phys. Chem. **36**, 621 (2017).

[3] A. Mauracher, O. Echt, A. M. Ellis, S. Yang, D. K. Bohme, J. Postler, A. Kaiser, S. Denifl, and P. Scheier, Phys. Rep. **751**, 1 (2018).

[4] C. F. Barenghi, R. J. Donnelly, and W. F. Vinen, *Quantized Vortex Dynamics and Superfluid Turbulence* (Springer, Berlin, 2001).

[5] L. Pitaevskii and S. Stringari, *Bose-Einstein Condensation and Superfluidity*, International Series of Monographs on Physics Vol. 164 (Oxford University Press, New York, 2016).

[6] L. F. Gomez, K. R. Ferguson, J. P. Cryan, C. Bacellar, R. M. P. Tanyag, C. Jones, S. Schorb, D. Anielski, A. Belkacem, C. Bernando, R. Boll, J. Bozek, S. Carron, G. Chen, T. Delmas, L. Englert, S. W. Epp, B. Erk. L. Foucar, R. Hartmann, A. Hexemer, M. Huth, J. Kwok, S. R. Leone, J. H. S. Ma, F. R. N. C. Maia, E. Malmerberg, S. Marchesini, D. M. Neumark, B. Poon, J. Prell, D. Rolles, B. Rudek, A. Rudenko, M. Seifrid, K. R. Siefermann, F. P. Sturm, M. Swiggers, J. Ullrich, F. Weise, P. Zwart, C. Bostedt, O. Gessner, and A. F. Vilesov, Science **345**, 906 (2014).

[7] C. L. Vicente, C. Kim, H. J. Maris, and G. M. Seidel, J. Low Temp. Phys. **121**, 627 (2000).

[8] See Supplemental Material at http://link.aps.org/supplemental/10.1103/PhysRevB.99.140505 for a fourfold movie showing simultaneously the time evolution of (a) the merging droplets represented by their sharp density surfaces (top left); (b) a two-dimensional view on a plane containing the incident direction as symmetry axis (top right); (c) pseudovorticity visualized by $|\nabla \times \mathbf{j}(\mathbf{r}, t)| = 10^{-3}$ Å^{-3} ps^{-1} isosurfaces (bottom left); and (d) compressible, incompressible, and total $\mathcal{E}_{\rm hyd}(k, t)$ (connected points) leading to the k scalings, superimposed to the static panels of Fig. 4 (bottom right).

[9] W. F. Vinen and J. J. Niemela, J. Low Temp. Phys. **128**, 167 (2002).

[10] *Progress in Low Temperature Physics*, edited by M. Tsubota and W. P. Halperin (Elsevier, Amsterdam/London, 2009), Vol. XVI.

[11] C. F. Barenghi, L. Skrbek, and K. P. Sreenivasan, Proc. Natl. Acad. Sci. USA **111**, 4647 (2014).

[12] M. Tsubota, K. Fujimoto, and S. Yui, J. Low Temp. Phys. **188**, 119 (2017).

[13] A. Villois and H. Salman, Phys. Rev. B **97**, 094507 (2018).

[14] N. G. Berloff and P. H. Roberts, J. Phys. A **34**, 81 (2001).

[15] T. Frisch, Y. Pomeau, and S. Rica, Phys. Rev. Lett. **69**, 1644 (1992).

[16] N. Navon, A. L. Gaunt, R. P. Smith, and Z. Hadzibabic, Nature (London) **539**, 72 (2016).

[17] M. Kobayashi and M. Tsubota, Phys. Rev. Lett. **94**, 065302 (2005).

[18] D. Proment, S. Nazarenko, and M. Onorato, Phys. Rev. A **80**, 051603(R) (2009).

[19] M. Pi, F. Ancilotto, F. Coppens, N. Halberstadt, A. Hernando, A. Leal, D. Mateo, R. Mayol, and M. Barranco, *4He-DFT BCN-TLS: A Computer Package for Simulating Structural Properties and Dynamics of Doped Liquid Helium-4 Systems*, https://github.com/bcntls2016/.

[20] F. Ancilotto, M. Barranco, F. Caupin, R. Mayol, and M. Pi, Phys. Rev. B **72**, 214522 (2005).

[21] D. E. Galli, L. Reatto, and M. Rossi, Phys. Rev. B **89**, 224516 (2014).

[22] I. Amelio, D. E. Galli, and L. Reatto, Phys. Rev. Lett. **121**, 015302 (2018).

[23] M. Barranco, R. Guardiola, S. Hernández, R. Mayol, J. Navarro, and M. Pi, J. Low Temp. Phys. **142**, 1 (2006).

[24] J. Eggers, J. R. Lister, and H. A. Stone, J. Fluid Mech. **401**, 293 (1999).

[25] B. Sun and M. S. Pindzola, J. Phys. B: At., Mol. Opt. Phys. **41**, 155302 (2008).

[26] G. Ferioli, G. Semeghini, L. Masi, G. Giusti, G. Modugno, M. Inguscio, A. Gallemí, A. Recati, and M. Fattori, Phys. Rev. Lett. **122**, 090401 (2019).

[27] M. Wu, T. Cubaud, and C.-M. Ho, Phys. Fluids **16**, L51 (2004).

[28] L. Duchemin, J. Eggers, and C. Josserand, J. Fluid Mech. **487**, 167 (2003).

[29] H. Roberts and J. Grant, J. Phys. A **4**, 55 (1971).

[30] S. Moroni, D. E. Galli, S. Fantoni, and L. Reatto, Phys. Rev. B **58**, 909 (1998).

[31] A. Cidrim, A. C. White, A. J. Allen, V. S. Bagnato, and C. F. Barenghi, Phys. Rev. A **96**, 023617 (2017).

[32] C. Nore, M. Abid, and M. E. Brachet, Phys. Fluids **9**, 2644 (1997).

[33] A. S. Bradley and B. P. Anderson, Phys. Rev. X **2**, 041001 (2012).

[34] M. T. Reeves, B. P. Anderson, and A. S. Bradley, Phys. Rev. A **86**, 053621 (2012).

[35] Note that the roton burst is very intense because the droplets are identical and so are the colliding ring/antiring. If they were not, one would expect the intensity to decrease. For large asymmetries, the rings might even cross without annihilating. Eventually, they should decay by interacting either with density modulations, as the small rings described here do, or with the droplet surface.

[36] J. Salort, C. Baudet, B. Castaing, B. Chabaud, F. Daviaud, T. Didelot, P. Diribarne, B. Dubrulle, Y. Gagne, F. Gauthier, A. Girard, B. Hébral, B. Rousset, P. Thibault, and P.-E. Roche, Phys. Fluids **22**, 125102 (2010).

[37] S. Nazarenko and M. Onorato, Physica D **219**, 1 (2006).

[38] A. Villois, G. Krstulovic, D. Proment, and H. Salman, J. Phys. A **49**, 415502 (2016).

[39] A. Freund, D. Gonzalez, X. Buelna, F. Ancilotto, and J. Eloranta, Phys. Rev. B **98**, 094520 (2018).

[40] Necessarily, at each chosen time, a segment of the closed circuit used to evaluate the circulation is in the low (but nonzero) density region extending beyond the sharp density surface. The contribution of this segment is needed to ascertain that the circulation is indeed quantized.

[41] C. R. Cabrera, L. Tanzi, J. Sanz, B. Naylor, P. Thomas, P. Cheiney, and L. Tarruell, Science **359**, 301 (2018).

[42] G. Semeghini, G. Ferioli, L. Masi, C. Mazzinghi, L. Wolswijk, F. Minardi, M. Modugno, G. Modugno, M. Inguscio, and M. Fattori, Phys. Rev. Lett. **120**, 235301 (2018).

[43] M. Klawunn and L. Santos, Phys. Rev. A **80**, 013611 (2009).